Modal effects on pump-pulse propagation in an Ar-filled capillary

Richard T. Chapman,[1] Thomas J. Butcher,[2] Peter Horak,[2,*] Francesco Poletti,[2] Jeremy G. Frey,[1] and William S. Brocklesby[2]

[1]*School of Chemistry, University of Southampton, Southampton SO17 1BJ, United Kingdom*
[2]*Optoelectronics Research Centre, University of Southampton, Southampton SO17 1BJ, United Kingdom*
*peh@orc.soton.ac.uk

Abstract: Accurate three-dimensional modelling of nonlinear pulse propagation within a gas-filled capillary is essential for understanding and improving the XUV yield in high harmonic generation. We introduce both a new model based on a multimode generalized nonlinear Schrödinger equation and a novel spatio-spectral measurement technique to which the model can be compared. The theory shows excellent agreement with the measured output spectrum and the spatio-spectral measurement reveals that the model correctly predicts higher order mode contributions to spectral broadening of the pulse. Fluorescence from the excited argon is used to verify the predicted ion distribution along the capillary.

OCIS codes: (190.7110) Ultrafast nonlinear optics; (080.1510) Propagation methods;

References and links

1. A. L'Huillier, and P. Balcou, "High-order harmonic generation in rare gases with a 1-ps 1053-nm laser," Phys. Rev. Lett. **70**(6), 774–777 (1993).
2. I. Christov, H. Kapteyn, and M. Murnane, "Quasi-phase matching of high-harmonics and attosecond pulses in modulated waveguides," Opt. Express **7**(11), 362–367 (2000).
3. I. P. Christov, M. M. Murnane, and H. C. Kapteyn, ""High-Harmonic Generation of Attosecond Pulses in the "single-cycle" Regime," Phys. Rev. Lett. **78**(7), 1251–1254 (1997).
4. I. P. Christov, "Control of high harmonic and attosecond pulse generation in aperiodic modulated waveguides," J. Opt. Soc. Am. B **18**(12), 1877–1881 (2001).
5. C. Courtois, A. Couairon, B. Cros, J. R. Marquès, and G. Matthieussent, "Propagation of intense ultrashort laser pulses in a plasma filled capillary tube: Simulations and experiments," Phys. Plasmas **8**(7), 3445–3456 (2001).
6. M. Nurhuda, A. Suda, M. Hatayama, K. Nagasaka, and K. Midorikawa, "Propagation dynamics of femtosecond laser pulses in argon," Phys. Rev. A **66**(2), 023811 (2002).
7. R. K. Nubling, and J. A. Harrington, "Launch conditions and mode coupling in hollow-glass waveguides," Opt. Eng. **37**(9), 2454–2458 (1998).
8. C. A. Froud, R. T. Chapman, E. T. F. Rogers, M. Praeger, B. Mills, J. Grant-Jacob, T. J. Butcher, S. L. Stebbings, A. M. de Paula, J. G. Frey, and W. S. Brocklesby, "Spatially resolved Ar * and Ar + * imaging as a diagnostic for capillary-based high harmonic generation," J. Opt. A, Pure Appl. Opt. **11**(5), 054011 (2009).
9. F. Poletti, and P. Horak, "Description of ultrashort pulse propagation in multimode optical fibers," J. Opt. Soc. Am. B **25**(10), 1645 (2008).
10. E. A. J. Marcatili, and R. A. Schmeltzer, "Hollow Metallic and Dielectric Waveguides for Long Distance Optical Transmission and Lasers," Bell Syst. Tech. J. **43**, 1783–1809 (1964).
11. F. Poletti, and P. Horak, "Dynamics of femtosecond supercontinuum generation in multimode fibers," Opt. Express **17**(8), 6134–6147 (2009).
12. V. S. Popov, "Tunnel and multiphoton ionization of atoms and ions in a strong laser field (Keldysh theory)," Phys.Usp. **47**(9), 855–885 (2004).

1. Introduction

High-power ultrashort laser pulses at near-infrared wavelengths propagating in gas-filled capillaries can form a compact source of extreme ultraviolet (XUV) and soft X-ray radiation by high-harmonic generation (HHG) [1]. Maximisation of the frequency conversion efficiency requires a detailed understanding of the radiation-atom interaction mechanism as well as the propagation properties of both the near-infrared pump in the presence of a partially ionized

gas, and of the generated XUV. Previous theoretical studies of capillary-based HHG by Christov et al. [2] have used numerical solutions of the 3-dimensional version of the scalar wave equation. This work focused on understanding attosecond pulse generation [3] and quasi phasematching within waveguides [4]. Experimentally measurable predictions of these theories have typically centred on the temporal profile of the pump and the harmonics generated. In this work, we focus on understanding the spectral and spatial distribution of the pump. We introduce a numerical model of pump pulse propagation based on a multimode generalized nonlinear Schrödinger equation. This model is verified firstly by simple measurement of the total output spectrum, a commonly used procedure [5,6] which only tests the summation over all modes. More stringent testing of the model is then demonstrated by measuring the spatio-spectral distribution of the output power in the far field, and by measuring the evolution of the ionization along the capillary length. Both of these are much more sensitive to nonlinear mode coupling than the summed spectral output.

2. Experimental configuration

The experimental setup is shown in Fig. 1. A 40 fs laser pulse centred at 790 nm, with a 1 kHz repetition rate, was coupled into a 70 mm long hollow capillary with internal diameter 150 µm using a 0.5 m plano-convex lens. The ratio of beam spot size, w, to capillary radius, a, was 0.64, giving optimum coupling into the lowest order, EH_{11}, mode [7]. The input pulse energy was varied between 378 and 840 µJ (corresponding to an intensity range of 2.8–6.3 x10^{14} Wcm^{-2}) by inserting reflective neutral density filters into the beam.

The central region of the capillary was filled with argon gas via a pair of 300 µm holes drilled 20 mm from either end of the 70 mm long capillary. Argon gas at pressures up to 200 mbar could be introduced into the system from a pressure-regulated supply. The capillary was mounted within a vacuum chamber kept at ~10^{-4} mbar. The overall gas pressure profile was calculated using computational fluid dynamics and can be approximated by a central 30 mm flat region with linear pressure gradients in the 20 mm regions at each end of the capillary.
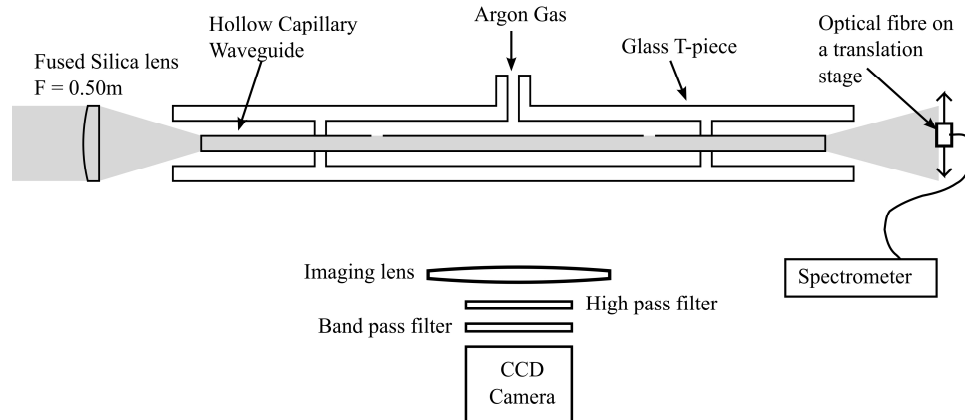

Fig. 1. Schematic for measuring the spatio-spectral output and argon ion fluorescence from a capillary running in a HHG regime.

The capillary output is a combination of the pump laser pulse and the generated XUV. The pump laser pulse was reflected out of the vacuum chamber into a fibre-coupled spectrometer mounted on a translation stage. The 125-µm diameter fibre end was placed at the centre of the beam and translated radially outwards across the whole beam profile. The argon ion fluorescence was imaged using the setup shown in Fig. 1, consisting of a 35 mm focal length lens imaging the capillary from the side onto a CCD. A high pass and bandpass filter were used to single out the 488 nm emission line that is emitted by singly ionised argon [8].

3. Numerical model

For the accurate theoretical description of the pump pulse propagation we developed a numerical model based on a multimode generalized nonlinear Schrödinger equation [9] which we extended to include ionization and plasma effects [5]. To this end, the electric field of the laser pulse is written as a sum over modal contributions

$$E(r,z,t) = \frac{\sqrt{2Z_0}}{2\pi} \sum_n \frac{1}{2} F_n(r) A_n(z,t) e^{i(k_0 z - \omega_0 t)} + c.c. \tag{1}$$

where $Z_0 = \sqrt{\mu_0 / \varepsilon_0}$, $F_n(r)$ is the transverse mode function of the EH_{1n} mode of the capillary [10] normalized to $\int rdr |F_n(r)|^2 = 1$, and A_n is the pulse envelope such that the modal power is given by $|A_n|^2 / (2\pi)$ in units of Watt, and the temporal dependence of the carrier wave has been factored out. Note that in writing Eq. (1) we have restricted the analysis to circularly symmetric modes only, assuming a symmetric pump laser mode and preferential coupling between modes of the same symmetry [9,11]. The modal evolution of the pulse along the capillary is then given by

$$\frac{\partial A_n}{\partial z} = iD_n + in_2(z)k_0 \sum_{k,l,m} Q_{nklm} A_k A_l A_l^* + \frac{i}{2} k_0 \int rdr F_n(r) S(r,z,t) n_{pl}^2(r,z,t)$$

$$- \frac{1}{2} \int rdr F_n(r) S(r,z,t) \frac{\rho_0(r,z,t) W(r,z,t) U}{|S(r,z,t)|^2 / (2\pi)} \tag{2}$$

Here, $S = \sum F_n A_n$, D_n describes modal dispersion and losses, including high-order dispersion, and the subsequent terms model the gas nonlinearity, plasma refractive index, and ionization losses of the pump, respectively. In Eq. (2), $n_2(z)$ is the nonlinearity of the neutral Ar gas as a function of the local pressure, k_0 is the propagation constant at the pump frequency, $Q_{nklm} = \int rdr F_n F_k F_l F_m$ are the mode overlap integrals, n_{pl} is the refractive index of the local plasma density resulting from ionization of the neutral gas by the propagating pulse, ρ_0 and W are the neutral gas density and ionization rate, respectively, and U is the ionization potential [5,9]. The ionization rate W is calculated using the Keldysh theory [12]. For the results presented in this work, the set of Eqs. (2) was solved by a Fourier split-step method for typically 20 modes, which we found sufficient for an accurate description of our experimental parameters. We emphasize that this model is capable of describing the full temporal dynamics of the propagating light in three dimensions, including modal effects such as group velocity mismatch. Therefore, as will be discussed in the following sections, the model allows us to investigate detailed spatial and spectral correlations, beyond what was possible with a simpler, earlier model [8].

4. Comparison of experimental results with numerical model

The predicted and measured total output spectra for three different input powers are shown in Fig. 2. The theoretical and experimental spectra show excellent agreement with not only the degree of blue shifting observed, but also the complex spectral shapes that occur at higher powers. We believe this is the first evidence that the blue-shifted shoulder of the spectrum is primarily located in higher order modes.
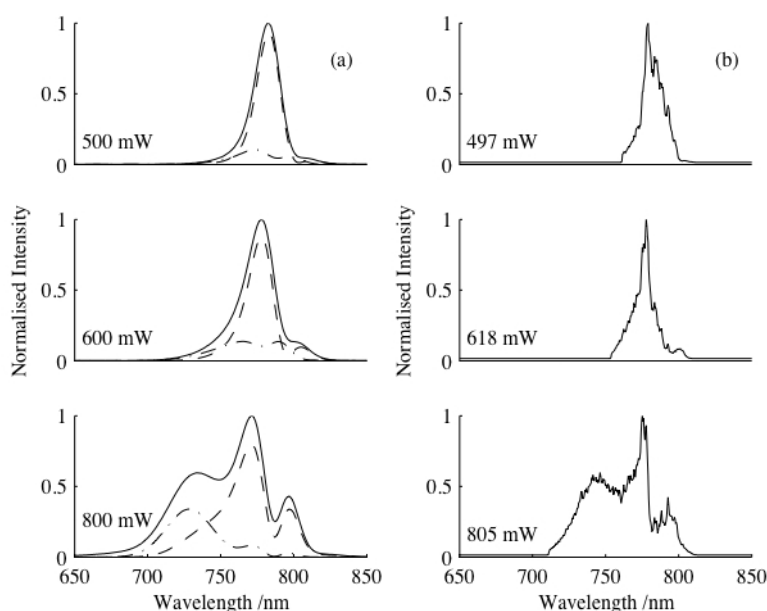
Fig. 2. Predicted (a) and experimental (b) output spectra measured for three input powers, shown. The predicted data shows the total spectrum (solid), as well as those for the EH_{11} (dashed) and EH_{12} (dot dashed) modes. At each laser power, the summed spectral intensity of the modes is normalised to a peak level of 1, as is the experimental data.

Figure 2 shows that at lower powers the EH_{11} mode dominates the spectrum as nonlinear mode coupling is small. The model also predicts a walk-off between the modes, this is calculated to be 8 fs between the EH_{11} and the EH_{12} modes along the 7 cm of the capillary. As the power is increased, more energy is coupled into the EH_{12} and other higher modes. The theoretical model indicates that nonlinear mode coupling is greater at the trailing edge of the pulse due to plasma defocusing, which leads to the observed blue shifted spectra in the higher order modes. Experimentally, the modal distribution cannot be directly determined from a summed spectrum of the kind shown in Fig. 2, although the agreement between theory and experiment allows us to infer that the modal distribution is correct.

In order to test whether the model correctly predicts the distribution of intensity in high order modes, we make use of the fact that as the modes propagate into the far field their spatial divergence is strongly dependent on their order, with higher order modes showing significantly greater angular spread. This means that the radial distribution of the spectral intensities has contributions from different modes at different radii (although the modes are not completely separated). Thus the spatio-spectral intensity distribution in the far field is very sensitive to any variation in the intensities of individual modes, and its measurement can provide a sensitive test of the ability of the numerical model to correctly predict the modal distribution.

Figure 3 shows the calculated (a) and measured (b) spectral intensity distribution as a function of radial distance from the beam axis. The theoretical intensity profiles of the EH_{11} and EH_{12} modes are shown for comparison. It is clear from both theoretical and experimental distributions that the differences in the intensity distributions of the modes are large. The EH_{11} mode has significant contributions at around 790 and 810 nm, and the blue-shifted components at about 740 nm show the same radial profile as the EH_{12} mode, with an on-axis peak, and another ~8 mm from the axis. This distribution is clear in the theoretically modelled intensity distribution. In the measured distributions, the general features of the pattern are

repeated. The EH_{11} mode appears at 780 and 810 nm, and the blue-shifted peak at 760 nm has the radially narrower distribution of the EH_{12} mode. However, several differences are clear. The first is that more extensive off-axis blue shifting is seen in the experimental data, implying greater broadening in the higher order modes than was predicted. Secondly, an extra peak can be seen close to the centre of the beam at ~800 nm in the experimental data. The shape of the EH_{11} peaks around 790-810 nm look similar to the spectral distortion caused by SPM, which produces first a splitting, and then a central peak, rising between the split peaks as the nonlinear phase shift increases. Both of these differences suggest that the nonlinear shifting of the spectrum is slightly stronger in the experiment than predicted by theory.
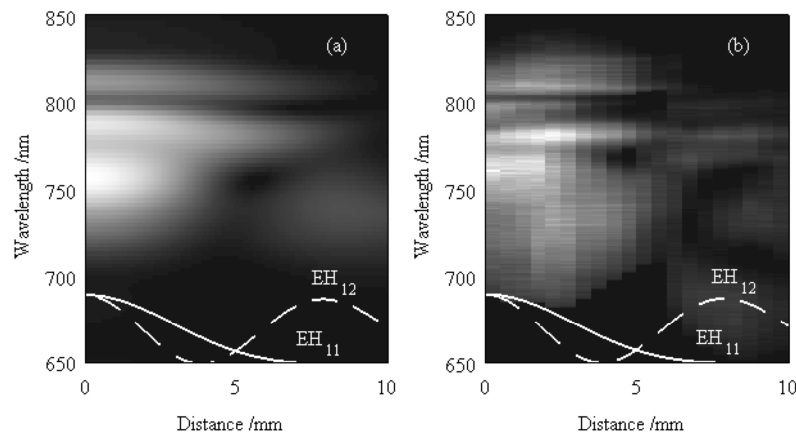

Fig. 3. Predicted (a) and experimental (b) spectral intensity plots in the lambda-r-plane. The solid and dashed white lines show the far-field profiles of the EH_{11} and EH_{12} modes respectively.

While spectral measurements at the capillary exit are a good test of the end point of the model, measurement of the Ar ion fluorescence along the length of the capillary provides a test of the model along the whole propagation length. Experimentally, the fluorescence, produced by excited Ar ions created by the pump pulse, is filtered and imaged from the side. The integrated fluorescence from each point along the capillary length can be compared directly to the ionisation levels predicted by the propagation model.

The integrated argon ion fluorescence and the theoretical integrated ionisation are compared in Fig. 4. The measured 488 nm argon ion fluorescence should be proportional to the calculated ionisation level within the capillary. The beat positions for the EH_{11} and EH_{12} modes calculated for linear propagation are shown as vertical dashed lines; as expected, both experimental and calculated beat positions are clearly shifted from these positions by the effects of nonlinear propagation. The initial increase in ionisation at the capillary entrance is observed in both theory and experiment and the first two major peaks appear at approximately the same positions within the capillary. The smaller structures within these major peaks do not correlate.
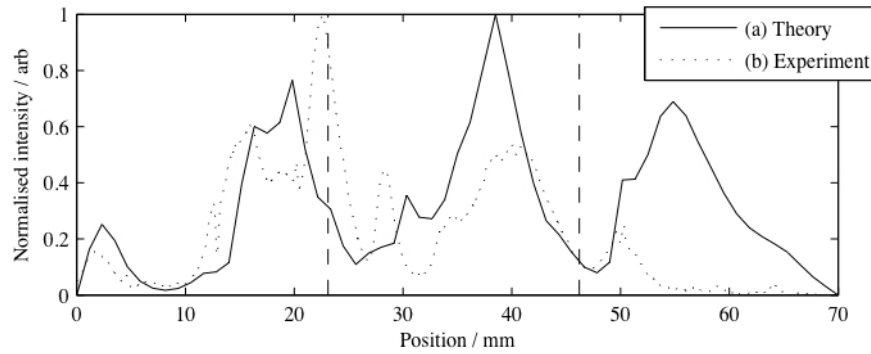
Fig. 4. Comparison of the summed radial ionisation (a) and the imaged argon ion fluorescence (b) along the length of the capillary. The vertical dashed lines show the beat positions for linear mode beating between the EH_{11} and EH_{12} modes.

The final major peak predicted by the numerical model is observed at the same point in the capillary but is significantly smaller in length and size. The discrepancy may be due to losses at the gas inlets within the capillary wall. These have been observed as increased scattering during experiments and are not included within the numerical model.

Conclusion

In this paper we have introduced a new method for numerically modelling nonlinear propagation within a capillary used for HHG. We have compared this model to the spectral output of the capillary and observed strong correlation. The model predicts the modal variation of the pulse shape, and the spatio-spectral measurement technique allows detailed comparison of not just the integrated spectrum, but also the individual modal contributions, because of the differences in the far-field mode patterns, validating the model and the coupling terms chosen. Understanding the modal distribution will allow modelling of XUV phase matching in the presence of nonlinear mode mixing, which is important for XUV generation at high intensities. It will also allow better understanding of the spatial profiles of the compressed pump pulses predicted by the model, providing a route to their exploitation.

Acknowledgments